Cell PRESS
Structure
Article

Site-Directed Mutagenesis Demonstrates the Plasticity of the β Helix: Implications for the Structure of the Misfolded Prion Protein

Jay H. Choi,[1] Barnaby C.H. May,[2,3] Cedric Govaerts,[4] and Fred E. Cohen[1,5,*]
[1]Department of Cellular and Molecular Pharmacology
[2]Department of Neurology
[3]Institute for Neurodegenerative Diseases
University of California, San Francisco, San Francisco, CA 94158, USA
[4]Structure et Fonction des Membranes Biologiques, Université Libre de Bruxelles, B-1050 Brussels, Belgium
[5]Department of Biochemistry and Biophysics, University of California, San Francisco, San Francisco, CA 94158, USA
*Correspondence: cohen@cmpharm.ucsf.edu
DOI 10.1016/j.str.2009.05.013

SUMMARY

The left-handed parallel β helix (LβH) fold has recently received attention as a possible structure for the prion protein (PrP) in its misfolded state. In light of this interest, we have developed an experimental system to examine the structural requirements of the LβH fold, using a known LβH protein, UDP-*N*-acetylglucosamine acyltransferase (LpxA), from *E. coli*. We showed that the β helix can tolerate nonhydrophobic residues at interior positions and prolines were important, but not critical, in folding of the β helix. Using our structural studies of the LβH, we threaded the sequence of the amyloidogenic fragment of the prion protein (residues 104–143) onto the structure of LpxA. Based on the threading result, we constructed the recombinant PrP-LpxA and tested its functional activity in an *E. coli* antibiotic sensitivity assay. The results of these experiments suggest that the amyloidogenic PrP fragment may fold into a β helix in the context of a larger β-helical structure.

INTRODUCTION

The parallel β helix is a repetitive protein fold where the repeating unit is a β-helical coil formed by segments of β strands (Choi et al., 2008; Iengar et al., 2006; Jenkins and Pickersgill, 2001). Each rung of the canonical β helix consists of two to three β strands interrupted by turn or loop regions (Iengar et al., 2006; Kajava and Steven, 2006; Simkovsky and King, 2006). The β-helical rungs are aligned to form a cross-β structure, such that elongated β sheets connected by hydrogen bonds run perpendicular to the helical axis (Choi et al., 2008; Govaerts et al., 2004; Simkovsky and King, 2006). The repetition of β helix coils creates a cylindrical hydrophobic core. The hydrophobic core of a β-helical protein is characterized by buried stacks of similar side chains (Choi et al., 2008; Jenkins and Pickersgill, 2001; Simkovsky and King, 2006). While right-handed β helices (RβH) are generally characterized by β strands connected by variable length turns and loops (Heffron et al., 1998; Iengar et al., 2006; Jenkins and Pickersgill, 2001), the right-handed β helix (LβH) is more rigid and repetitive than the RβH variant (Choi et al., 2008; Iengar et al., 2006; Jenkins and Pickersgill, 2001).

It has been proposed that misfolded proteins associated with neurodegenerative diseases, such as prion disease, may adopt an LβH fold (Govaerts et al., 2004; Langedijk et al., 2006; Stork et al., 2005; Wille et al., 2002; Yang et al., 2005). Recent solid-state nuclear magnetic resonance (NMR) studies of the fungal HET-s prion protein showed that the misfolded amyloid conformation may adopt an architecture that is structurally unrelated to the native conformations, but that is similar to a β helix or β solenoid fold (Kajava and Steven, 2006; Wasmer et al., 2008). Hence, it is plausible that mammalian prion proteins may also adopt β-helical architecture in the misfolded state.

Misfolded amyloid proteins share common structural characteristics, even when the native proteins are evolutionarily or structurally unrelated. Amyloid fibrils are generally unbranched, protease-resistant filaments with dominant β sheet structures organized in a cross-β fashion in which the β strands run perpendicular to the fibril axis (Jimenez et al., 2002; Murali and Jayakumar, 2005; Serpell et al., 2007). Previous prion amyloid modeling studies have converged on the β-helical architecture due to the structural features that β-helical folds share with the unresolved structure of longer chain amyloids. It has also been observed that expression of the isolated β-helical domain of the RβH protein, P22 tailspike protein, readily forms amyloid-like fibers (Schuler et al., 1999). Therefore, understanding the role of amino acid sequence in the folding of β helices may provide insight into how misfolded proteins could form elongated β sheet structures.

E. coli UDP-N-acetylglucosamine acyltransferase (LpxA) was the first example of a protein where an LβH is the predominant secondary structure (Raetz and Roderick, 1995). LpxA is a soluble, cytoplasmic protein that catalyzes the first step in the biosynthesis of lipid A, the hydrophobic anchor of lipopolysaccharides in gram-negative bacteria (Galloway and Raetz, 1990; Wyckoff and Raetz, 1999). Lipid A is required for the growth of *E. coli* and most other gram-negative bacteria and is also necessary for maintaining the integrity of the outer membrane as a barrier to toxic chemicals (Galloway and Raetz, 1990; Vaara, 1993). LpxA monomers are composed of a single β-helical domain, capped at the C terminus with an α-helical domain; they assemble into a homotrimer to form the active enzyme.

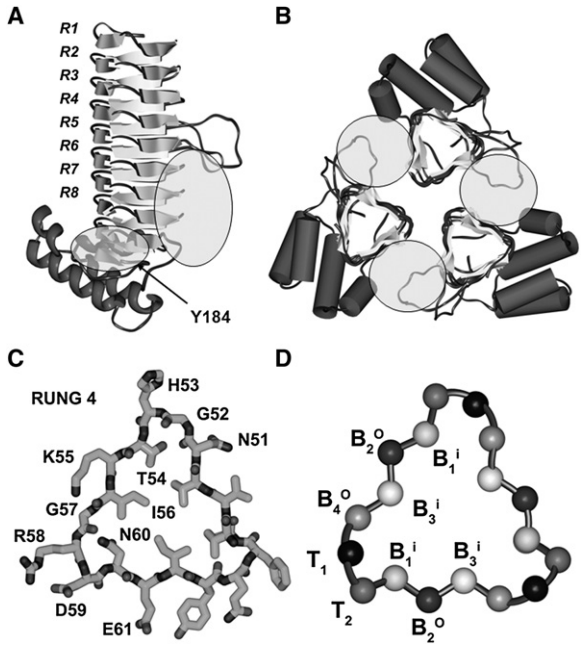

Figure 1. Monomeric and Trimeric Forms of the LβH Protein LpxA

(A) LpxA monomer structure (PDB ID: 1LXA) with labels at each rung. β-helical, loop, and α-helical domains are shown. The ligand binding site is indicated by the shaded circle. A tyrosine residue (Y184) at the bottom region of β-helical domain is indicated.

(B) Cross-sectional view of the LpxA trimer. The ligand binding site is indicated by the shaded circle.

(C) Cross-sectional view of the fourth rung of the LpxA β-helical domain. The residues of the identified targeted region for the LpxA in vivo folding assay (residues 51–62) are indicated.

(D) Cross-sectional view of the LpxA β-helical domain. The turn (T) and β sheet (B) with the superscript "i" for a residue facing inside and "o" for a residue facing outside.

The β-helical domain of LpxA contains approximately ten rungs (or coils) with two loop excursions (Figure 1). Three repeats of imperfect hexapeptide motifs ([LIV]-[GAED]-X_2-[STAV]-X) make up one rung of the β helix (Raetz and Roderick, 1995). Each rung of the canonical β helix consists of three flat and untwisted parallel β strands connected by either a one- or two-residue turn or a long loop excursion region (Choi et al., 2008; Iengar et al., 2006; Jenkins and Pickersgill, 2001; Kajava and Steven, 2006). Previous studies have shown defined residue distributions at the various positions of the repeats: each β strand contains small, uncharged residues (A, S, T, and C) and conserved, larger hydrophobic residues (L, I, and V) that face the interior of the LβH to create a hydrophobic core (Choi et al., 2008; Iengar et al., 2006; Jenkins and Pickersgill, 2001; Kajava and Steven, 2006). These constraints on the interior positions of the β strands are presumed to have restricted sequence variation of the LβH proteins throughout evolution (Parisi and Echave, 2001). The LβH fold is highly regular and symmetrical with little variability in shape or size over the length of the domain (Zheng et al., 2007). These features also have led to the suggestion that LβH fold may be used as a building block for nanotubular structures with application in nanotechnology (Haspel et al., 2006, 2007; Zanuy et al., 2007a; Zheng et al., 2007). With this interest, there have also been recent studies to improve the stability of the β helix structure using conformationally constrained amino acids (Ballano et al., 2008; Zanuy et al., 2007b). Despite growing interest in the LβH, there has been little structural characterization of the LβH fold. The accuracy of amyloid modeling studies using the LβH fold has been limited by the relative absence of information pertaining to the sequence requirements and structural features of this relatively rare protein fold.

In the present study, we investigated the folding and stability of the LpxA protein to examine the structural requirements of the LβH fold by altering the sequence in the β-helical domain. We showed that some nonhydrophobic residues could be tolerated at interior positions of the β helix and that proline residues were important, but not critical, in folding of the β helix. We designed a recombinant PrP-LpxA protein, in which a PrP fragment that is thought to be essential for the conformational conversion was incorporated into the β-helical domain of LpxA. Partial enzymatic activity was observed, suggesting that the β-helical structure may be able to accommodate a portion of the PrP sequence and, as a corollary, that a PrP fragment may adopt LβH architecture.

RESULTS

In Vivo Functional Assay to Study Folding of β Helices in LpxA

We developed a bioassay to evaluate the structural integrity of LpxA using LpxA enzymatic activity. The *E. coli* strain SM101 is deficient in LpxA activity due to a G189S inactivating mutation (glycine being the only residue allowed at position 189) in the chromosomal gene (Galloway and Raetz, 1990; Odegaard et al., 1997). This strain is defective in lipid A biosynthesis and is temperature sensitive, showing no growth at 37°C. At its permissive growth temperature of 30°C, SM101 displays hypersensitivity to antibiotics such as novobiocin, rifampin, and erythromycin that are normally excluded by the outer membrane (Odegaard et al., 1997; Vuorio and Vaara, 1992). When SM101 is transformed with plasmids containing the wild-type *lpxA* gene, normal growth is restored (Galloway and Raetz, 1990). Therefore, enzymatic activity of any LpxA mutant can be directly tested in a transformed SM101 strain exposed to various concentrations of antibiotics.

We constructed pJC1 (His tag LpxA) and pJC2 (His tag LpxA mutant containing a single tyrosine) plasmids as described in the Experimental Procedures. pJC1 contained the gene for wild-type LpxA, while pJC2 contained the gene for LpxA, where all tyrosine residues except one were substituted with either phenylalanine or histidine (Y66F, Y77F, Y219F, Y223F, and Y243H). pJC2 had a relatively uncomplicated spectroscopic signature, facilitating the characterization of the folded and unfolded states. Negative control mutants were made by site-directed mutagenesis at H125A and I86R of *lpxA* to generate mutant pJC2-H125A and pJC2-I86R, respectively. H125 is an important residue in the LpxA active site and its mutation almost completely eliminates LpxA activity (Williams and Raetz, 2007; Wyckoff and Raetz, 1999). The I86 residue is located in the fifth rung of the β-helical domain in the hydrophobic core of a β helix (Figure 1A). Based on our examination of the structure, a substitution at I86 with a large, charged residue, such as arginine, was targeted to promote improper folding or destabilization of the

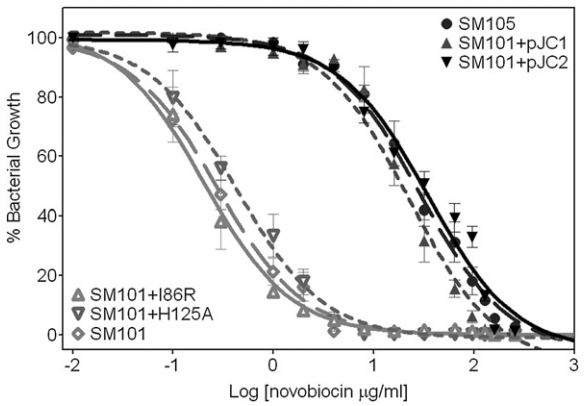

Figure 2. LpxA In Vivo Folding Assay at 30°C

LpxA folding assay (novobiocin: 0–256 μg/ml) showing bacterial growth of the SM105 and SM101 *E. coli* strains and SM101 (DE3) *E. coli* strain transformed with pJC1, pJC2, pJC2-H125A, and pJC2-I86R. Error bars are calculated from three experimental trials.

β-helical domain and thereby decrease LpxA activity of the pJC2-I86R mutant. Hence, H125A (pJC2-H125A) was used as a functional negative control mutant and I86R (pJC2-I86R) was used as a structural negative control mutant. Both mutants were used to test whether an LpxA functional assay could be used as an in vivo folding assay for β-helical folding.

The SM101 (DE3) strain was transformed with pJC1, pJC2, pJC2-H125A, and pJC2-I86R plasmids. Selected colonies of each transformant and SM105 (isogenic wild-type strain of SM101) were grown overnight, then transferred to 96 well plates and grown in medium dosed ampicillin (50 μg/ml), streptomycin (30 μg/ml), and novobiocin (0–256 μg/ml) at 30°C. Novobiocin was used to determine the antibiotic susceptibility of the SM101 (DE3) strain once transformed with either wild-type LpxA or the mutant plasmids. Bacterial growth was quantified after 12 hr by measuring the optical density at 600 nm (OD_{600}) and expressed as a function of novobiocin concentration. Introduction of the wild-type *lpxA* gene allowed *E. coli* containing the *lpxA2* mutation to grow under the same range of novobiocin concentrations as SM105. As shown in Figure 2, the single tyrosine mutant construct, pJC2, also showed growth similar to wild-type *E. coli*. Therefore, pJC2 was used as a wild-type LpxA control in the present study. In contrast, pJC2-H125A and pJC2-I86R showed significant reductions in growth and hypersensitivity to novobiocin (minimum inhibitory concentration of 4 μg/ml versus 256 μg/ml for wild-type). This result was consistent with previous studies of SM101 (Vuorio and Vaara, 1992). Note that no isopropyl β-D-1-thiogalatopyranoside (IPTG) induction was required, as the basal protein expression was sufficient to recover LpxA activity. Protein expression was verified by western blot using an anti-his antibody (data not shown).

Mutagenesis Target Selection

We first aimed at identifying the best site to probe structural requirements of the LβH in LpxA, i.e., where structural perturbations will lead to a functional phenotype. Therefore we conducted an arginine scan of the β-helical domain by site-directed mutagenesis at hydrophobic residues in the β-helical core, located in rungs 1–7 (Figure 1A). An in vivo folding assay with

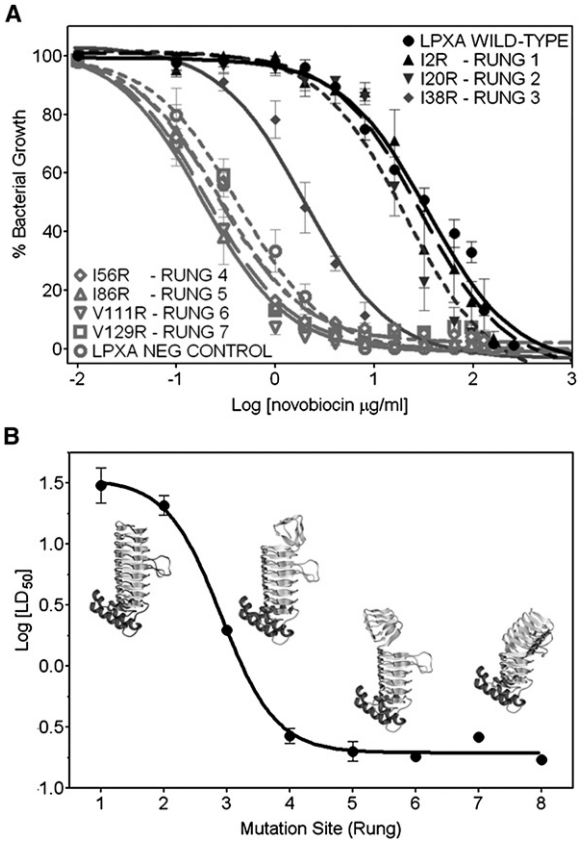

Figure 3. LpxA In Vivo Folding Assay for Wild-Type LpxA and Arginine LpxA Mutants at 30°C

(A) LpxA folding assay (novobiocin: 0–256 μg/ml) showing bacterial growth of the SM101 (DE3) *E. coli* strain transformed with wild-type LpxA, LpxA-H125A, or LpxA arginine mutants (I2R, I20R, I38R, I56R, I86R, V111R, and V129R). Hydrophobic residues at the B^{i}_{3} position were mutated in the LpxA arginine mutants. (B) Average log (LD_{50}) of each arginine LpxA mutant for three trials of the LpxA in vivo folding assay, showing the large difference between the LpxA-I20R and LpxA-I56R mutants.

Error bars are calculated from three experimental trials.

novobiocin was conducted at 30°C with the LpxA mutants I2R, I20R, I38R, I56R, I86R, V111R, and V129R along with controls, as described earlier (Figure 3A). The log LD_{50} (50% of the lethal dose concentration) was calculated from the bacterial growth curve plotted against the novobiocin concentration. Log LD_{50} was then plotted against the location of mutagenesis sites, referenced by rung number (Figure 3B). The arginine scan of the hydrophobic core of the β-helical domain showed that LpxA can be fully or partially active, even with the disruption of up to three rungs (I38R) of the β-helical domain. However, an arginine mutation at I56 eliminated the activity of LpxA. Therefore, based on our arginine scan and structural analysis of the active site, we identified a region of rung 4 (residues 51–62) as an ideal target for studying the folding and stability of the β-helical region.

Site-Directed Mutagenesis in the Hydrophobic Core of the β-Helical Domain

In order to study the effect of nonhydrophobic residues in the core of the β-helical region on LpxA folding, we conducted

site-directed mutagenesis at residue I56, substituting with alanine, asparagine, glutamine, glycine, and arginine. SM101 (DE3) was transformed with the LpxA mutants and the in vivo folding assay was performed at 30°C. The assay was also conducted at 37°C in order to test whether SM101 (DE3) transformed with LpxA mutants could restore *E. coli* growth and to compare the effect of mutations on LpxA folding at a normal growth temperature. Wild-type LpxA and negative control (LpxA-H125A) mutants were also characterized in the in vivo folding assay. At 30°C, substitution of I56 with alanine did not significantly affect the in vivo LpxA activity, but glycine, asparagine, and glutamine mutations showed lower LpxA activity than the wild-type. The arginine mutant was completely inactive (Figure 4A). At 37°C, wild-type, alanine, asparagine, glutamine, and glycine mutations showed similar levels of LpxA activity within the range of standard deviation, but their LpxA activities at 37°C were decreased by 2- to 4-fold compared to those at 30°C. The arginine mutants showed complete loss of LpxA activity at 37°C (Figure 4B).

To assess these results at the level of protein expression, LpxA mutants were individually overexpressed using IPTG induction at 30°C. Soluble and insoluble fractions of the lysates were separated by centrifugation and the samples were analyzed by electrophoresis on an SDS polyacrylamide gel. As can be seen in Figure 4C, wild-type LpxA, LpxA-H125A, and the alanine and asparagine LpxA mutants were found mostly in the soluble fractions. Weaker LpxA bands were observed from the soluble fractions of lysates from the glutamine mutant bacteria. LpxA from the glycine and arginine mutant bacteria were found mostly in the insoluble fraction, indicating that the arginine mutation had a detrimental effect on folding of the β helix. Although the expression level of soluble glycine LpxA mutant was lower than expected from the LpxA in vivo folding assay, protein expression of the LpxA mutants was consistent overall with the LpxA in vivo folding assay.

Proline Mutagenesis at the Turn Regions of the β-Helical Domain

Surveys of known LβH structures indicate that proline residues are restricted to defined positions, suggesting a possible role in folding and stability (Choi et al., 2008). To investigate any possible role for prolines in folding and stability, two proline residues (P28 and P34) and four proline residues (P10, P28, P34, and P183) at the T_1 positions of the β-helical domain were replaced with alanine using site-directed mutagenesis. These were termed PtoA-2 and PtoA-4, respectively. The P182 residue, which is located in the unusual turn position of B^{o}_{4}, was excluded from our scanning, due to its deleterious effect on LpxA folding when mutated to glycine or alanine (data not shown). Results from the in vivo folding assay showed that the activity of the PtoA-4 mutant was lower than wild-type LpxA, but still greater than the negative control, LpxA-H125A. The PtoA-2 mutant showed greater activity than the PtoA-4 mutant (Figure 5A).

Unfolding and Refolding of LpxA Monitored by Tyrosine Fluorescence

The thermodynamic stability of the wild-type and proline LpxA mutant was probed by tyrosine fluorescence spectroscopy. We used a modified LpxA background where all but a single tyrosine

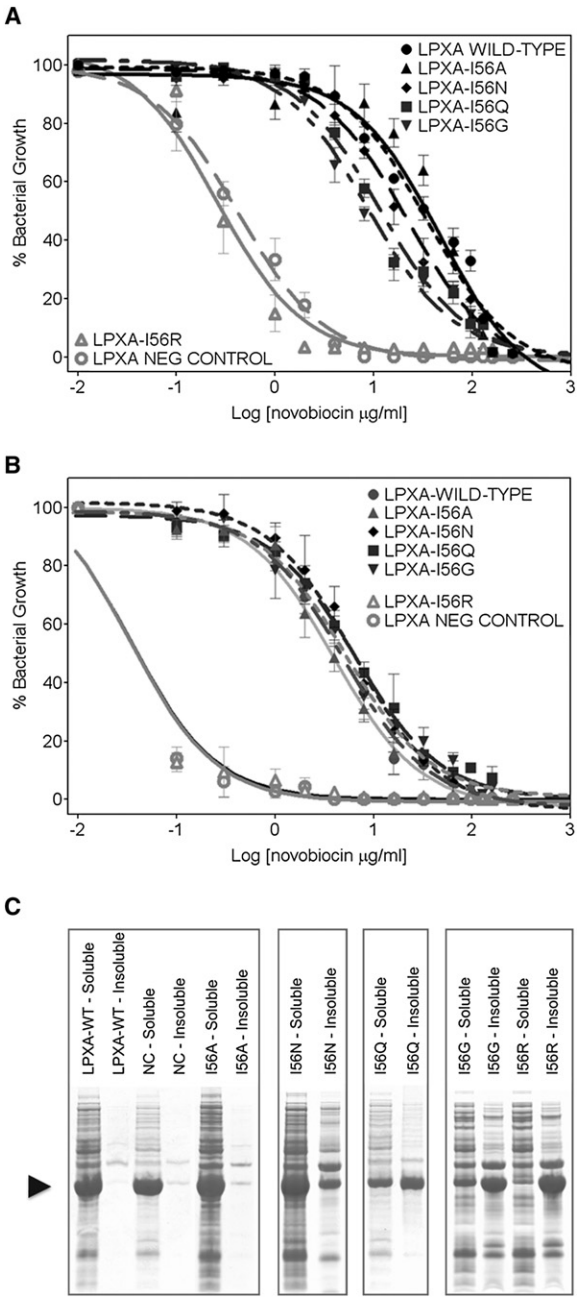

Figure 4. In Vivo Folding Assay for LpxA Mutants with Mutations in the Hydrophobic Core

(A and B) LpxA folding assay, showing bacterial growth of the SM101 (DE3) *E. coli* strain, transformed with LpxA containing one of the following mutations: (A) At 30°C, LpxA wild-type (LD_{50} = 34 ± 1.5 μg/ml), LpxA-H125A negative control (LD_{50} = 0.42 ± 1.0 μg/ml), I56A (LD_{50} = 46 ± 2.3 μg/ml), I56N (LD_{50} = 22 ± 1.8 μg/ml), I56Q (LD_{50} = 12 ± 1.5 μg/ml), I56G (LD_{50} = 8.6 ± 1.7 μg/ml), and I56R (LD_{50} = 0.27 ± 1.3 μg/ml); (B) At 37°C, LpxA wild-type (LD_{50} = 5.0 ± 1.6 μg/ml), LpxA-H125A negative control (LD_{50} = 0.034 ± 1.1 μg/ml), I56A (LD_{50} = 3.9 ± 1.5 μg/ml), I56N (LD_{50} = 6.4 ± 1.9 μg/ml), I56Q (LD_{50} = 6.5 ± 1.8 μg/ml), I56G (LD_{50} = 5.2 ± 1.7 μg/ml), and I56R (LD_{50} = 0.034 ± 1.2 μg/ml). (C) SDS polyacrylamide gel electrophoresis of soluble and insoluble fractions of overexpressed LpxA cellular lysates is shown. Arrow indicates monomer bands of LpxA and LpxA mutant proteins.

Error bars are calculated from three experimental trials.

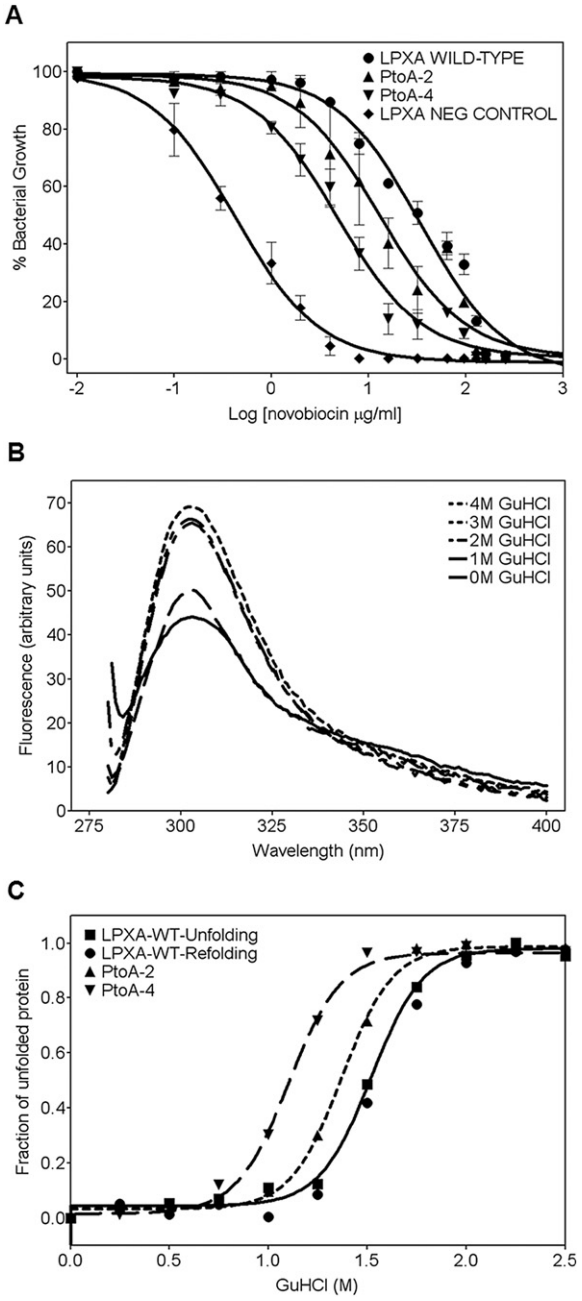

Figure 5. In Vivo Folding Assay and Spectroscopic Characterization of Wild-Type LpxA and LpxA Proline Mutants

(A) The functional activity of LpxA mutants with two and four prolines replaced by alanine residues in the β-helical domain PtoA-2 (LD_{50} = 13 ± 3.2 μg/ml) and PtoA-4 (LD_{50} = 4.8 ± 1.7 μg/ml) at 30°C.

(B) Fluorescence emission spectra of LpxA in its native state (solid line) and in its GdnHCl-denatured states (dotted line) were recorded in 100 mM sodium phosphate (pH 7.5), containing 0–4 M GdnHCl.

(C) The folding and unfolding transition of wild-type LpxA and LpxA mutant proteins. Transitions were measured using fluorescence (emission at 303 nm) after 30 min incubation. Uncorrected fluorescence emission spectra were recorded with a Spex Fluoromax (excitation at 275 nm, spectral bandwidth of 3 nm [excitation] and 3 nm [emission]). All spectra were recorded at 25°C and are buffer-corrected. The protein concentrations were 100 μg/ml. Error bars are calculated from three experimental trials.

residue (Y184) were replaced with phenylalanine or histidine in order to simplify the fluorescence spectrum during folding and unfolding. As Y184 is protected from the solvent by the C-terminal domain, unfolding of the protein will lead to increased exposure of Y184 that will translate into increased fluorescence intensity. The mutant proteins were expressed and purified, as described in the Experimental Procedures section. Upon excitation at 280 nm, maximal fluorescent emission was observed at 303 nm (Figure 5B), which as expected increased in intensity upon addition of the denaturant, guanidine hydrochloride (GdnHCl), and subsequent protein unfolding. To determine whether LpxA unfolding induced by a chemical denaturant is reversible, GdnHCl-induced folding and unfolding of LpxA was monitored by measuring the tyrosine fluorescence spectra (Figure 5C). Denaturation and renaturation curves were superimposable, both with $[GdnHCl]_{1/2}$ concentrations of 1.5 M. Only a single state transition was observed and no trimer assembly was detected, indicating that the change in fluorescence spectra reflects changes of the monomer structure. To determine whether proline mutations in the β-helical domain affect the thermodynamic stability of LpxA, the unfolding transition of the PtoA-2 and PtoA-4 mutants were monitored over a range of GdnHCl concentrations. As shown in Figure 5C, denaturation of the PtoA-2 and PtoA-4 mutants occurred at lower denaturation concentrations compared to the wild-type, with $[GdnHCl]_{1/2}$ concentrations of approximately 1.3 M and 1.1 M GdnHCl, respectively.

Residue Tolerance in the β-Helical Domain

A selected target region of the β-helical domain (residues 51–62) was further studied by determining the amino acid residue tolerance at each position (Figures 1C and 1D). Based on our in vivo and in vitro folding analysis of LpxA mutants, we selected concentrations of novobiocin (4–8 μg/ml) to measure viable LpxA activity at 30°C. We performed site-directed mutagenesis at all six β helix positions (T_1, T_2, B^i_1, B^o_2, B^i_3, and B^o_4), introducing, one at a time, residues that were not observed at these positions in known structures of LβH. More specifically leucine, valine, and tryptophan were tested at position T_1; isoleucine and valine at position T_2; glycine, asparagine, serine, and glutamine and methionine, arginine, lysine, tryptophan, tyrosine, histidine, glutamate, aspartate, and proline at positions B^i_1 and B^i_3; and aspartate and proline at B^o_2 and B^o_4. LpxA mutants were transformed into SM101 (DE3) and grown under novobiocin selection at 30°C. Table 1 summarizes the allowed and disallowed amino acid residues for each position of the β helix, as well as residues that have been observed at each position, based on sequence analysis (Choi et al., 2008). Any LpxA mutant strain that grew under the selection criteria was considered a viable mutant and the amino acid residue introduced in the mutant was categorized as "allowed." While proline residues are restricted to only T_1 and T_2 positions, as expected from the previous study (Choi et al., 2008), glycine and hydrophilic residues, such as asparagine and glutamine, that were not previously seen in the β-helical core were shown to be tolerated at B^i_1 and B^i_3 positions.

Inclusion of a PrP Fragment into the β-Helical Domain of Recombinant LpxA

Our LpxA assay provides a simple way to test whether an amyloid-forming peptide can adopt an LβH architecture. Based

Table 1. Amino Acid Residue Tolerance of LpxA LβH Domain from the In Vivo LpxA Folding Assay

Type	Position	Known[a]	Allowed	Not Allowed
T_1	G52, R58	P, D, G, A, E, N, S, H, K, T, Y, M, F, R, Q, I, C	L, V, W	
T_2	H53, D59	N, G, D, P, F, R, E, K, Q, H, S, Y, T, L, A, M, W, C	I, V	
B^i_1	T54, N60	V, A, T, S, C, I, N, L, F	G, Q, M	R, K, W, Y, H, E, D, P
B^o_2	K55, E61	V, T, I, S, E, Y, K, F, H, R, M, N, W, L, Q, A, G, C	D	P
B^i_3	I56, I62	I, V, L, A, F, T, M, C	G, N, Q, S	R, K, W, Y, H, E, D, P
B^o_4	G57, N51	G, E, A, D, H, V, N, S, I, K, R, M, T, L, Y, Q, C, F, W		P

[a] Values were taken from the multiple sequence alignment of LpxA and other LβH proteins (Choi et al., 2008) and listed in order of occurrence frequency. Amino acid residues tested and newly observed to be tolerated (Allowed) and not tolerated (Not Allowed) at each position of β helix domain of LpxA. In vivo LpxA folding assay was conducted at 30°C with 4–8 μg/ml of novobiocin as a selection concentration.

on the observed residue tolerance at each position of the LpxA β helix, we threaded fragments of mouse PrP (residues 104–143) onto a target region of LpxA that we probed earlier to determine whether it is possible for this PrP sequence to fold into a β helix. Combining previous studies (Choi et al., 2008; Govaerts et al., 2004), and results from the present study (Table 1), the sequence threading and modeling was conducted based on the following criteria: proline residues are only allowed at the T_1 and T_2 positions, the B^i_1 position will only tolerate small residues, while relatively large hydrophobic residues will be favored at position B^i_3. The restriction of glycine to some B^o_4 positions was also considered. The threading result (Figure 6A) shows a reasonable sequence alignment between mouse PrP sequence (PrP residues 104–143) and the LpxA sequence (LpxA residues 22–59), with the exception of a short loop region (PrP residues 134–135). While glycine and alanine residues were placed at several B^i_1 and B^i_3 positions, proline residues were placed at T_1 positions in order to meet the criteria. The modeling results also show a reasonable structural alignment and packing of the interiors of the β helix in PrP-LpxA models (see Figure S1 available online). However, the substitutions with residues of small side chains, such as glycine and alanine, resulted in loose packing of the hydrophobic core, which may contribute to the destabilization of the β helix structure.

A synthesized fragment of the prion gene was incorporated into the *lpxA* gene following the sequence threading. LpxA monomer structure with the target region for PrP fragment is shown in Figure 6B. The prion fragment 104–143 was subcloned into the corresponding region of *lpxA* in the pJC2 plasmid (replacing residues 22–29), and the resulting construct was then transformed into SM101 (DE3) and tested for LpxA activity. In order to facilitate proper assembly of the required trimeric LpxA structure, two residues involved in the trimeric interface of LpxA (F29 and H47) were retained in PrP-LpxA. To ensure that the region into which the PrP sequence was inserted is sensitive to the in vivo folding assay we constructed the LpxA-V48R+T54R mutant. This mutant contained arginine mutations in the region where the PrP sequence was inserted. This first chimeric PrP-LpxA construct as well as the LpxA-V48R+T54R mutant negative control were both inactive in the in vivo assay (data not shown). Thus, a second chimeric construct was prepared to include four more residues from LpxA (i.e., G39 at B^o_4, T42 at B^i_1, T54 at B^i_3, and I56 at B^i_3). Those residues were selected since they were speculated to be highly conserved due to the steric constraints on the particular region of the LpxA β-helical domain. As shown in Figure 6C, this pseudo PrP-LpxA recombinant protein showed a substantial increase in activity, albeit lower than that of the wild-type. Importantly, the same construct with the additional V48R and T54R disrupting mutations did not show any LpxA activity, indicating that the enzyme is completely disrupted upon strong perturbation of the β helix and therefore that the activity of the pseudo PrP-LpxA protein is not provided by a partly misfolded enzyme. These results suggest that the PrP 104-143 fragment may adopt a β-helical architecture in the context of the chimera (see Discussion).

DISCUSSION

The LpxA assay developed here offers an indirect but simple way to probe the relationship between sequence and structure of LβH. The interest is 2-fold. First it provides an experimental tool to test whether residue propensities and distributions, as identified by database surveys (Choi et al., 2008), fully define the LβH or if the fold can accept more variations than those observed in known structures and sequences. Second, considering the proposed role of LβH architectures in amyloid formation, it offers an experimental method to test whether amyloid-prone sequences can adopt a β-helical structure.

Glycine and Hydrophilic Residues in the Hydrophobic Core of the β Helix

Site-directed mutagenesis of the identified target region and subsequent in vivo folding assays showed that the LpxA β helix tolerates more residue types in the hydrophobic core than expected from database surveys. For example, sequence analysis of LβH proteins has shown strong conservation of hydrophobic residues, such as isoleucine, leucine, and valine at B^i_3 (Choi et al., 2008; Iengar et al., 2006). In contrast, the current in vivo folding study has demonstrated that a single substitution with hydrophilic residues, such as asparagine and glutamine, can still be tolerated by the β helix. In the case of glycine at B^i_3, some activity is maintained, albeit decreased relative to the wild-type.

A decrease in the antibiotic resistance of the viable mutants could either be due to a decrease in specific activity of the LpxA mutant or to a decrease in the expression of the mutant. An SDS-PAGE analysis of the expression profile of the various LpxA mutants showed that a decrease in activity correlated with an accumulation of the protein in the insoluble fraction. This suggests that the destabilizing mutations affected the folding efficiency, rather than specific activity (although a culmination of both effects cannot be excluded). This was particularly

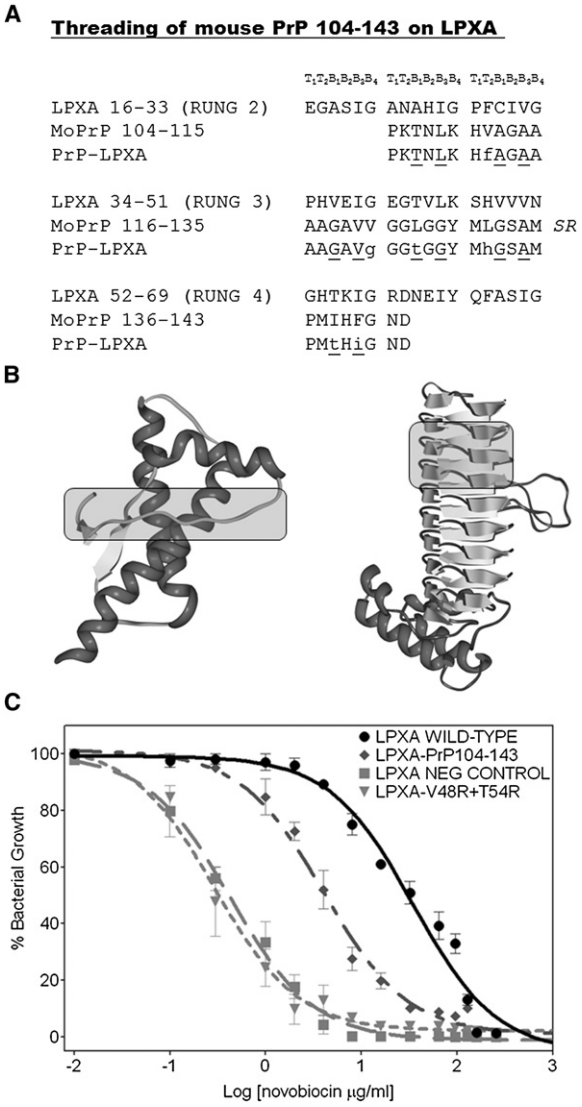

Figure 6. Threading the PrP Sequence onto the LpxA Protein and In Vivo Folding Assay of the PrP-LpxA Recombinant Protein

(A) Threading of mouse PrP (residues 104–143) onto LpxA (residues 22–59). PrP-LpxA is a chimeric protein where residues 22–59 of LpxA are replaced by a modified PrP fragment (residues 104–143). Mutations are indicated by lowercase letters. PrP residues (S134 and R135) that were not threaded onto LpxA are indicated in italics. Residues at interior positions B_1^i and B_3^i are indicated by underlined letters.

(B) Native PrP structure (PDB ID: 1QM0; residues 125–228). The PrP region (residues 124–143) used in the LpxA threading is indicated by the shaded rectangle. LpxA monomer structure (PDB ID: 1LXA) with the target region for PrP fragment insertion in the β-helical domain is indicated by the shaded rectangle.

(C) LpxA in vivo folding assay of PrP-LpxA (LD_{50} = 4.1 ± 1.3 μg/ml) and the control mutant, LpxA-V48R+T54R (LD_{50} = 0.29 ± 1.2 μg/ml), at 30°C. Error bars are calculated from three experimental trials.

striking when charged side chains were placed inside the protein core, such as for the I56R mutant, where the protein is found exclusively in insoluble inclusion bodies.

The results are overall consistent with an alanine site-directed mutagenesis study of the RβH, P22 tailspike protein (Simkovsky and King, 2006), such that the conserved hydrophobic residues at the interior positions are important in folding of the β helix. However, our results also revealed that LpxA can tolerate point mutations with residues, such as glycine and glutamine at B^i_3 positions, which were previously considered to be critical in β-helical folding. The fact that glutamines and asparagines are allowed at interior positions of LpxA is particularly interesting knowing that the LβH fold has been proposed as a putative architecture for polyglutamine amyloid fibers (Chopra et al., 2008; Govaerts et al., 2004). Indeed, such models require the presence of glutamine side chains both on the outside and, importantly, in the interior of the β helix.

The Effect of Proline Mutations on the Thermodynamic Stability of the LβH Protein

Using the intrinsic tyrosine fluorescence spectrum we measured the thermodynamic stability of LpxA ($[GdnHCl]_{1/2}$ = 1.5 M GdnHCl), which was in close agreement to the RβH domain of the P22 tailspike protein reported by Schuler et al. (1999). In order to accurately monitor protein denaturation and renaturation using fluorescence, we have constructed the single tyrosine LpxA mutant, which contained a tyrosine residue at position 184. Y184 is located near the edge of the β helix and α helix domain, away from the trimeric interface, and therefore the decrease in fluorescence intensity observed most likely does not reflect separation of the trimer, but rather monomer denaturation. In addition, the shift in the denaturation curves observed upon mutation of prolines, which are located further up the β helix, indicates that we measured global protein denaturation and not solely an increase of solvent exposure of Tyr 184.

As previously described (Choi et al., 2008), prolines in the β-helical domain are mostly located at the top and bottom region of the domain, leading us to speculate that they may play an important role in the initiation or termination of β-helical folding. Due to the unique structural properties, proline often plays a key role in the protein structure. The effect of incorporating a conformationally constrained amino acid residue, such as proline and proline analogues, into a peptide chain has been extensively studied (Flores-Ortega et al., 2008). Our current result shows that β-helical folding occurs without the proline residues, but the LpxA activity is substantially reduced. Based on the LpxA sequence and structure, the proline residues targeted for alanine substitution were not located in the active site, nor are they expected to be involved in trimer formation. Therefore, the reduced LpxA activity of the proline mutants can best be explained by the decreased thermodynamic stability of the β helix, as indicated by unfolding transitions monitored using tyrosine fluorescence spectroscopy in the presence of a chemical denaturant. Proline mutations of the β helix may also have an effect on the efficiency of β-helical folding. However, in order to accurately determine the folding efficiency of the β helix, folding kinetics of the wild-type and other mutant proteins need to be investigated further.

PrP-LpxA Hybrid Recombinant Protein Supports the β-Helical Model of PrP^{Sc}

Recent structural studies using microcrystals of amyloid forming short peptides have suggested that fibrillar assemblies have their origins in steric zippers, tightly packed β-structures of both parallel and anti-parallel nature (Nelson et al., 2005; Sawaya et al., 2007; Wiltzius et al., 2008). While the biological relevance

of these short peptides is a matter of debate, recent solid state NMR and electron microscopy studies of Aβ amyloid fibrils have shown in-register parallel β structures (Petkova et al., 2002; Sachse et al., 2008).

In the case of mammalian prions, a number of recent studies suggest that the misfolded state may adopt a β-solenoid or β-helical architecture (Govaerts et al., 2004; Langedijk et al., 2006; Wasmer et al., 2008; Yang et al., 2005). The inherent compactness and availability of accessible β faces to initiate and sustain self-assembly make β-helical folds attractive candidates for the structural unit of the prion amyloid fibril. Previous modeling studies of PrP^{Sc} showed that the protein could adopt two to four rungs of the β-helical fold (Govaerts et al., 2004; Langedijk et al., 2006; Yang et al., 2005). However, questions have been raised about the validity of these β-helical models of PrP^{Sc} because PrP contains sequence features that do not match sequences of known β-helical proteins. While the insolubility of PrP^{Sc} has limited structural studies to test the models by classical techniques, such as X-ray crystallography and NMR spectroscopy, the short fragments known to be prone to amyloid formation (De Gioia et al., 1994; Forloni et al., 1993; Gasset et al., 1992; Thellung et al., 2000) can be threaded and experimentally tested using a recombinant LβH protein containing a PrP-derived amyloidogenic fragment. This chimeric protein was used to investigate the possibility of a β-helical structure in the misfolded prion protein conformation.

Although results from the in vivo functional assay showed that the PrP-LpxA recombinant protein had LpxA activity comparable to other LpxA mutants, it may not provide sufficient evidence to conclude that the PrP misfolds into a β helix. First, the PrP fragment in the PrP-LpxA recombinant protein contained several residues that were different from the wild-type prion. In the PrP-LpxA recombinant protein, wild-type LpxA residues were maintained for trimeric interface residues, a conserved glycine residue at B^{o}_{4} position, and three interior residues at B^{i}_{1} and B^{i}_{3} positions for the following reasons. Residues involved in the trimeric interaction may not be critical to β-helical folding, but they may destabilize the formation of LpxA trimer, leading to a false negative result for the in vivo folding assay. The B^{o}_{4} position can accommodate a range of different residues, but it is often highly conserved as a glycine residue due to steric constraints. Isoleucine and phenylalanine have been observed at interior positions B^{i}_{1} and B^{i}_{3}. However, the packing of these residues with other wild-type residues in the targeted region of LpxA β-helical domain may not be compatible.

In addition, interpretation of the in vivo folding assay results for PrP-LpxA is still somewhat problematic as the recombinant protein did not exhibit wild-type-like LpxA activity. First, one could suspect that LpxA could have accommodated a PrP-like sequence in a non-β-helical-like structure (such as a loop) while maintaining enzymatic activity. However, our arginine scanning has demonstrated that structural perturbation in the third helical rung strongly affects function while perturbation of the fourth rung completely abrogated enzymatic activity. Our chimeric construct integrated the PrP-like sequence in place of rung 2, 3, and 4 of LpxA with only moderate effect on enzymatic activity. This suggests that the overall architecture had been preserved in the vicinity of the fourth rung. In addition, accommodating a 40 residue segment into a non-β-helical structure should be quite unfavorable to LpxA folding and assembly, especially considering the tightness of the trimerization interface of the enzyme. A possibility would be that PrP-LpxA β-helical folding may occur, but in a less stable form than in wild-type LpxA. Overexpression of the PrP-LpxA recombinant protein was attempted under several conditions, but insoluble aggregates are often formed under the induced conditions, hampering biophysical characterization of the PrP-LpxA recombinant protein. Further studies are necessary to explore expression conditions that will allow examination of the structure and biophysical characteristics of the PrP-LpxA recombinant protein and may lead to a better understanding of PrP structure.

While the PrP sequence becomes relatively insoluble when it adopts a β-rich structure, we believed that if the sequence could be grafted successfully onto a sequence known to form a water soluble trimeric LβH fold, we would create a useful tool for studying PrP structure. As many features could limit the success of the hybrid design, the negative result is of limited utility. For example, the specific misfolded PrP structure could deviate locally from that of known β-helical proteins, such as fungal HET-s prion protein, or it could disrupt the solubility of the chimeric construct. Therefore, it may be difficult to directly test the full-length β-helical model of PrP^{Sc} on known soluble β-helical proteins that facilitate spectroscopic characterization. For these reasons, we focused on a β-rich segment of the prion protein (PrP 103–143) and retained two LpxA residues that were involved in the trimeric interface and four that played structural roles. We believe that the ability of the hybrid to fold sufficiently to yield enzymatic activity suggests that a central region of PrP may adopt a β-helical structure. However, the tendency of this hybrid to aggregate suggests that the intrinsic solubility of the β helix with the PrP sequence is difficult to preserve.

EXPERIMENTAL PROCEDURES

Bacterial Strains

Bacterial strains SM105 (*lpxA*, $Strep^{r}$) and SM101 (*lpxA2*, $Strep^{r}$) (Galloway and Raetz, 1990) were obtained from the *E. coli* Genetic Stock Center (Yale University, New Haven, Connecticut). SM101 (DE3) was prepared from SM101 using the Lambda DE3 lysogenization kit (Novagen) and made electrocompetent for transformation (Ausubel, 1987).

Site-Directed Mutagenesis

LpxA mutants were made by using the PCR-based QuikChange mutagenesis procedure (Stratagene). Five tyrosine residues of LpxA were subjects to site-directed mutagenesis in order to generate recombinant LpxA with a single tyrosine. The resulting vector that contained the single tyrosine wild-type LpxA clone, pJC2, encoded the full-length LpxA protein with the following mutations: Y66F, Y77F, Y219F, Y223F, and Y243H. For all other LpxA mutants, methylated pJC2 DNA was used as a template DNA for site-directed mutagenesis. A PCR reaction was carried out with forward and reverse primers, using *Pfu* polymerase. The cycle was: 94°C for 30 s, 55°C for 1 min, and 62°C for 10 min. This cycle was repeated 18 times. Plasmid DNA was purified using QIAprep Spin MiniPrep kits (QIAGEN). DNA sequencing of an 800 bp region containing the targeted codon confirmed mutant clones (Elim Biopharmaceuticals). Primers for mutagenesis and the *PrP-LpxA* recombinant gene were custom made by Celtek Bioscience and Integrated DNA Technologies.

LpxA In Vivo Folding Assay

Previously prepared SM101 (DE3) electrocompetent cells were transformed with pJC2 vectors, containing the single tyrosine wild-type and mutant LpxA clones using a Gene Pulser Xcell Electroporator (Bio-Rad). Transformants were plated on LB agar containing appropriate antibiotics (100 μg/ml ampicillin

and 30 μg/ml streptomycin) and incubated at 30°C. Colonies were picked and inoculated in LB medium (100 μg/ml ampicillin and 30 μg/ml streptomycin) and incubated for 12 hr at 30°C. Two microliters of diluted overnight inoculums were mixed in each well of 96 well plates, prepared with LB medium (100 μg/ml ampicillin, 30 μg/ml streptomycin, and 0–256 μg/ml novobiocin). The 96 well plates were incubated on a shaker at 30°C for 12 hr and at 37°C for 6 hr. The OD_{600} was recorded using a SpectraMax M5 microplate reader (Molecular Device).

Protein Expression and Purification

LpxA and LpxA mutant proteins were expressed in SM101 (DE3) cells. LpxA transformed cells were grown in LB medium (100 μg/ml ampicillin and 30 μg/ml streptomycin) at 15 to 30°C until OD_{600} = 0.8. Cells were induced with 0.5 mM of IPTG and grown for another 12 hr. Cell suspensions were centrifuged and cell pellets were collected and lysed. Cell lysates were centrifuged at 15,000 rpm for 30 min to collect the soluble fraction. The pellets were collected and resuspended in 8 M urea as insoluble fractions. For the in vitro folding and unfolding study, the soluble proteins were purified using the Ni-NTA purification system (QIAGEN) and size-exclusion chromatography. The wild-type LpxA protein eluted as a 90 kDa protein, indicating that LpxA mostly exists as a trimer in solution. Around 15 mg of purified protein was obtained from 1 liter of bacterial culture. The collected protein samples were separated on SDS polyacrylamide gels for verification of the LpxA monomer (28 kDa).

In Vitro Folding and Unfolding (Tyrosine Fluorescence Spectroscopy)

Folding transitions were measured in a Spex FluoroMax spectrofluorometer (HORIBA Jobin Yvon, Inc.) with a thermostated cell holder using plastic fluorescence cuvettes. The excitation wavelength was 280 nm and the emission wavelengths were 280–400 nm. For unfolding transitions, cold buffer (100 mM sodium phosphate [pH 7.5], containing 0.2 M NaCl and 1 mM EDTA) was first mixed with 10 μl of concentrated protein solution (10 mg/ml). Then, a cold, concentrated GdnHCl solution containing 100 mM sodium phosphate (pH 7.5), 0.2 M NaCl, and 1 mM EDTA was added (final volume 1 ml) to a final protein concentration of 100 μg/ml. For refolding transitions, 4 M GdnHCl solution was added and the samples were incubated for 30 min. Refolding was initiated by rapid dilution with buffer containing 0.2 M NaCl and 1 mM EDTA.

Sequence Threading and Molecular Modeling of PrP-LpxA

The models of PrP-LpxA were built on the template of LpxA N-terminal domain (PDB ID code: 1LXA) by following the selected threading of mouse PrP (residues 104–143) onto LpxA (residues 22–59). While the backbone chains of LpxA were maintained, the side chains of the LpxA sequence (residues 22–59) were replaced with PrP sequence using Insight II software (Accelrys). The side chain positions of the PrP-LpxA models were subsequently optimized using SCWRL 3.1 (Canutescu et al., 2003). Models were further optimized using two rounds of energy minimization using the GROMACS 3.1.3 package (Van Der Spoel et al., 2005).

SUPPLEMENTAL DATA

Supplemental data include Supplemental Experimental Procedures and one figure and can be found with this article online at http://www.cell.com/structure/supplemental/S0969-2126(09)00226-3.

ACKNOWLEDGMENTS

We thank Robert Fletterick, Anthony Lau, and Holger Wille for valuable discussions and critically reading the manuscript and Christian R.H. Raetz for providing us with pTO1 vector. This research was supported by National Institutes of Health grant AG21601.

Received: March 3, 2009
Revised: April 20, 2009
Accepted: May 16, 2009
Published: July 14, 2009

REFERENCES

Ausubel, F.M. (1987). Current Protocols in Molecular Biology (Brooklyn, NY: John Wiley and Sons, Inc.).

Ballano, G., Zanuy, D., Jimenez, A.I., Cativiela, C., Nussinov, R., and Aleman, C. (2008). Structural analysis of a beta-helical protein motif stabilized by targeted replacements with conformationally constrained amino acids. J. Phys. Chem. B *112*, 13101–13115.

Canutescu, A.A., Shelenkov, A.A., and Dunbrack, R.L., Jr. (2003). A graph-theory algorithm for rapid protein side-chain prediction. Protein Sci. *12*, 2001–2014.

Choi, J.H., Govaerts, C., May, B.C., and Cohen, F.E. (2008). Analysis of the sequence and structural features of the left-handed beta-helical fold. Proteins *73*, 150–160.

Chopra, M., Reddy, A.S., Abbott, N.L., and de Pablo, J.J. (2008). Folding of polyglutamine chains. J. Chem. Phys. *129*, 135102.

De Gioia, L., Selvaggini, C., Ghibaudi, E., Diomede, L., Bugiani, O., Forloni, G., Tagliavini, F., and Salmona, M. (1994). Conformational polymorphism of the amyloidogenic and neurotoxic peptide homologous to residues 106-126 of the prion protein. J. Biol. Chem. *269*, 7859–7862.

Flores-Ortega, A., Jimenez, A.I., Cativiela, C., Nussinov, R., Aleman, C., and Casanovas, J. (2008). Conformational preferences of alpha-substituted proline analogues. J. Org. Chem. *73*, 3418–3427.

Forloni, G., Angeretti, N., Chiesa, R., Monzani, E., Salmona, M., Bugiani, O., and Tagliavini, F. (1993). Neurotoxicity of a prion protein fragment. Nature *362*, 543–546.

Galloway, S.M., and Raetz, C.R. (1990). A mutant of *Escherichia coli* defective in the first step of endotoxin biosynthesis. J. Biol. Chem. *265*, 6394–6402.

Gasset, M., Baldwin, M.A., Lloyd, D.H., Gabriel, J.M., Holtzman, D.M., Cohen, F., Fletterick, R., and Prusiner, S.B. (1992). Predicted α-helical regions of the prion protein when synthesized as peptides form amyloid. Proc. Natl. Acad. Sci. USA *89*, 10940–10944.

Govaerts, C., Wille, H., Prusiner, S.B., and Cohen, F.E. (2004). Evidence for assembly of prions with left-handed beta-helices into trimers. Proc. Natl. Acad. Sci. USA *101*, 8342–8347.

Haspel, N., Zanuy, D., Aleman, C., Wolfson, H., and Nussinov, R. (2006). De novo tubular nanostructure design based on self-assembly of beta-helical protein motifs. Structure *14*, 1137–1148.

Haspel, N., Zanuy, D., Zheng, J., Aleman, C., Wolfson, H., and Nussinov, R. (2007). Changing the charge distribution of beta-helical-based nanostructures can provide the conditions for charge transfer. Biophys. J. *93*, 245–253.

Heffron, S., Moe, G.R., Sieber, V., Mengaud, J., Cossart, P., Vitali, J., and Jurnak, F. (1998). Sequence profile of the parallel beta helix in the pectate lyase superfamily. J. Struct. Biol. *122*, 223–235.

Iengar, P., Joshi, N.V., and Balaram, P. (2006). Conformational and sequence signatures in beta helix proteins. Structure *14*, 529–542.

Jenkins, J., and Pickersgill, R. (2001). The architecture of parallel beta-helices and related folds. Prog. Biophys. Mol. Biol. *77*, 111–175.

Jimenez, J.L., Nettleton, E.J., Bouchard, M., Robinson, C.V., Dobson, C.M., and Saibil, H.R. (2002). The protofilament structure of insulin amyloid fibrils. Proc. Natl. Acad. Sci. USA *99*, 9196–9201.

Kajava, A.V., and Steven, A.C. (2006). Beta-rolls, beta-helices, and other beta-solenoid proteins. Adv. Protein Chem. *73*, 55–96.

Langedijk, J.P., Fuentes, G., Boshuizen, R., and Bonvin, A.M. (2006). Two-rung model of a left-handed beta-helix for prions explains species barrier and strain variation in transmissible spongiform encephalopathies. J. Mol. Biol. *360*, 907–920.

Murali, J., and Jayakumar, R. (2005). Spectroscopic studies on native and protofibrillar insulin. J. Struct. Biol. *150*, 180–189.

Nelson, R., Sawaya, M.R., Balbirnie, M., Madsen, A.O., Riekel, C., Grothe, R., and Eisenberg, D. (2005). Structure of the cross-beta spine of amyloid-like fibrils. Nature *435*, 773–778.

Odegaard, T.J., Kaltashov, I.A., Cotter, R.J., Steeghs, L., van der Ley, P., Khan, S., Maskell, D.J., and Raetz, C.R. (1997). Shortened hydroxyacyl chains on lipid A of *Escherichia coli* cells expressing a foreign UDP-N-acetylglucosamine O-acyltransferase. J. Biol. Chem. *272*, 19688–19696.

Parisi, G., and Echave, J. (2001). Structural constraints and emergence of sequence patterns in protein evolution. Mol. Biol. Evol. *18*, 750–756.

Petkova, A.T., Ishii, Y., Balbach, J.J., Antzutkin, O.N., Leapman, R.D., Delaglio, F., and Tycko, R. (2002). A structural model for Alzheimer's beta-amyloid fibrils based on experimental constraints from solid state NMR. Proc. Natl. Acad. Sci. USA *99*, 16742–16747.

Raetz, C.R., and Roderick, S.L. (1995). A left-handed parallel beta helix in the structure of UDP-N-acetylglucosamine acyltransferase. Science *270*, 997–1000.

Sachse, C., Fandrich, M., and Grigorieff, N. (2008). Paired beta-sheet structure of an Abeta(1-40) amyloid fibril revealed by electron microscopy. Proc. Natl. Acad. Sci. USA *105*, 7462–7466.

Sawaya, M.R., Sambashivan, S., Nelson, R., Ivanova, M.I., Sievers, S.A., Apostol, M.I., Thompson, M.J., Balbirnie, M., Wiltzius, J.J., McFarlane, H.T., et al. (2007). Atomic structures of amyloid cross-beta spines reveal varied steric zippers. Nature *447*, 453–457.

Schuler, B., Rachel, R., and Seckler, R. (1999). Formation of fibrous aggregates from a non-native intermediate: the isolated P22 tailspike beta-helix domain. J. Biol. Chem. *274*, 18589–18596.

Serpell, L.C., Benson, M., Liepnieks, J.J., and Fraser, P.E. (2007). Structural analyses of fibrinogen amyloid fibrils. Amyloid *14*, 199–203.

Simkovsky, R., and King, J. (2006). An elongated spine of buried core residues necessary for in vivo folding of the parallel beta-helix of P22 tailspike adhesin. Proc. Natl. Acad. Sci. USA *103*, 3575–3580.

Stork, M., Giese, A., Kretzschmar, H.A., and Tavan, P. (2005). Molecular dynamics simulations indicate a possible role of parallel beta-helices in seeded aggregation of poly-Gln. Biophys. J. *88*, 2442–2451.

Thellung, S., Florio, T., Corsaro, A., Arena, S., Merlino, M., Salmona, M., Tagliavini, F., Bugiani, O., Forloni, G., and Schettini, G. (2000). Intracellular mechanisms mediating the neuronal death and astrogliosis induced by the prion protein fragment 106-126. Int. J. Dev. Neurosci. *18*, 481–492.

Vaara, M. (1993). Antibiotic-supersusceptible mutants of *Escherichia coli* and *Salmonella typhimurium*. Antimicrob. Agents Chemother. *37*, 2255–2260.

Van Der Spoel, D., Lindahl, E., Hess, B., Groenhof, G., Mark, A.E., and Berendsen, H.J. (2005). GROMACS: fast, flexible, and free. J. Comput. Chem. *26*, 1701–1718.

Vuorio, R., and Vaara, M. (1992). The lipid A biosynthesis mutation lpxA2 of *Escherichia coli* results in drastic antibiotic supersusceptibility. Antimicrob. Agents Chemother. *36*, 826–829.

Wasmer, C., Lange, A., Van Melckebeke, H., Siemer, A.B., Riek, R., and Meier, B.H. (2008). Amyloid fibrils of the HET-s(218-289) prion form a beta solenoid with a triangular hydrophobic core. Science *319*, 1523–1526.

Wille, H., Michelitsch, M.D., Guenebaut, V., Supattapone, S., Serban, A., Cohen, F.E., Agard, D.A., and Prusiner, S.B. (2002). Structural studies of the scrapie prion protein by electron crystallography. Proc. Natl. Acad. Sci. USA *99*, 3563–3568.

Williams, A.H., and Raetz, C.R. (2007). Structural basis for the acyl chain selectivity and mechanism of UDP-N-acetylglucosamine acyltransferase. Proc. Natl. Acad. Sci. USA *104*, 13543–13550.

Wiltzius, J.J., Sievers, S.A., Sawaya, M.R., Cascio, D., Popov, D., Riekel, C., and Eisenberg, D. (2008). Atomic structure of the cross-beta spine of islet amyloid polypeptide (amylin). Protein Sci. *17*, 1467–1474.

Wyckoff, T.J., and Raetz, C.R. (1999). The active site of *Escherichia coli* UDP-N-acetylglucosamine acyltransferase. Chemical modification and site-directed mutagenesis. J. Biol. Chem. *274*, 27047–27055.

Yang, S., Levine, H., Onuchic, J.N., and Cox, D.L. (2005). Structure of infectious prions: stabilization by domain swapping. FASEB J. *19*, 1778–1782.

Zanuy, D., Rodriguez-Ropero, F., Haspel, N., Zheng, J., Nussinov, R., and Aleman, C. (2007a). Stability of tubular structures based on beta-helical proteins: self-assembled versus polymerized nanoconstructs and wild-type versus mutated sequences. Biomacromolecules *8*, 3135–3146.

Zanuy, D., Rodriguez-Ropero, F., Nussinov, R., and Aleman, C. (2007b). Testing beta-helix terminal coils stability by targeted substitutions with non-proteogenic amino acids: a molecular dynamics study. J. Struct. Biol. *160*, 177–189.

Zheng, J., Zanuy, D., Haspel, N., Tsai, C.J., Aleman, C., and Nussinov, R. (2007). Nanostructure design using protein building blocks enhanced by conformationally constrained synthetic residues. Biochemistry *46*, 1205–1218.